Proceedings of the
10th Graz Brain-Computer Interface Conference 2026 10.3217/978-3-99161-093-9-031

Why Simple Models Still Matter: Adaptive sLDA for Non-Stationary EEG Decoding

J. Egger[1] and G. R. Müller-Putz[1,2]

[1] Institute of Neural Engineering, Graz University of Technology, Graz, Austria
[2] BioTechMed Graz, Austria

E-mail: gernot.mueller@tugraz.at

ABSTRACT: Electroencephalography (EEG)-based brain-computer interfaces (BCIs) are strongly affected by non-stationarities, causing covariate shifts between calibration and deployment and leading to performance degradation over time. While deep learning approaches address this issue, they typically require large training datasets that are often unavailable in practical BCI scenarios. We therefore investigate lightweight online adaptation strategies for shrinkage linear discriminant analysis (sLDA), a simple yet robust classifier for low-data EEG settings. We evaluate three unsupervised methods: exponential moving average feature normalization (*FNorm*), pooled mean adaptation of the classifier bias (*PMean*), and pooled mean with covariance adaptation (*PMean+Cov*). Across six sessions from 20 participants, without FP/min control, true-positive rates rose by 14.27% (*FNorm*), 29.13% (*PMean*) and 5.87% (*PMean+Cov*), while false-positives per minute changed to 3.71 (+2.19) for *FNorm*, 11.95 (+10.44) for *PMean*, and 1.05 (-0.47) for *PMean+Cov* (not statistically significant). *PMean+Cov* achieved the best balance between sensitivity and false positives, making it most suitable for real-time BCI speller applications.

INTRODUCTION

Locked-in syndrome is a condition in which individuals remain fully conscious but lose most voluntary motor control, severely limiting communication [1]. Within the INTRECOM project, we develop a fully implantable brain-computer interface (BCI) for real-time motor and speech decoding to enable home-based communication, particularly via a speller interface. As the implantable system is still under development, non-invasive electroencephalography (EEG) provides a practical platform to investigate decoding strategies, adaptation mechanisms, and real-time constraints. In this context, reliable control and low false-positive rates (FPR) are crucial, as unintended activations directly impair usability and increase user frustration.

A key challenge in EEG-based decoding is non-stationarity, which induces covariate shifts [2] between calibration (training) and deployment (test) data due to changes in e.g., cognition or feedback [3-5]. Although deep learning [6,7] and domain adaptation methods [8,9] address this problem, they often rely on larger datasets and higher computational resources than linear models, limiting their suitability for short-calibration BCI settings. Adaptive extensions of linear discriminant analysis (LDA) have therefore been widely studied [10-14]. Here, we build on shrinkage LDA (sLDA) without modifying its shrinkage structure, preserving its robustness to low signal-to-noise ratios, inter-channel correlations, and limited training data in high-dimensional EEG [15,16]. The novelty of our approach lies in extending sLDA with lightweight online adaptation while retaining its regularization framework.

We propose three online adaptation strategies: (1) exponential moving average (EMA) for feature normalization to track distributional shifts, a model-agnostic approach applicable beyond sLDA, (2) pooled mean adaptation to update the classifier bias while keeping weights fixed, building on prior LDA-based work [10,12], and (3) pooled mean and covariance adaptation to update, which updates both bias and classifier weights and represents the main methodological contribution, extending covariance adaptation to the shrinkage LDA while preserving its regularization structure under limited data conditions. To our knowledge, such an adaptation has not been previously investigated for sLDA in BCI settings. These methods enable efficient online adaptation with minimal complexity while explicitly controlling FPR for real-time speller application.

This work focuses on a controlled comparison within the sLDA framework to isolate the effect of lightweight adaptation under identical model complexity. A direct comparison to alternative adaptive models in terms of data efficiency and computational cost is beyond the scope of this study and remains subject to future work.

We hypothesize that lightweight online adaptation of sLDA improves classification performance under non-stationary conditions while maintaining low FPRs, making it suitable for real-time speller applications.

MATERIALS AND METHODS

A. Dataset

The dataset [17] in use comprised hand gesture recordings from 22 healthy right-handed adults (20-40 years). EEG was recorded with 60 active gel-based

10.3217/978-3-99161-093-9-031

electrodes (actiCAP, Brain Products GmbH, Germany) placed according to the 10-10 system and four EOG electrodes for artifact correction (500 Hz sampling rate). A synchronized video motion capture system tracked a marker on the right index finger to determine movement onset. Participants completed six sessions between 2 p.m. and midnight, spaced two hours apart, including cognitive tasks, a standardized meal, and fatigue-inducing activities. Each session contained an eye movement paradigm for artifact correction [18] and a cue-based task with four right-hand gestures (fist, pistol, pincer, and the "Y" sign in American Sign Language). Each session consisted of eight runs, yielding 64 trials per gesture per participant. Two participants were excluded due to incomplete data.

B. *Processing of recordings*

Signal processing and decoding was performed in Python. Raw EEG data were visually inspected, and noisy channels were interpolated using spherical splines [19]. Powerline noise (50 Hz and harmonics) was removed with a 2nd-order IIR Butterworth comb filter, followed by a non-causal 0.3-70 Hz 4th-order Butterworth bandpass filter. Eye artifacts were removed using the SGEYESUB algorithm [18] trained on a separate eye-movement dataset. Signals were low-pass filtered at 3 Hz, down-sampled to 16 Hz (f_s), and re-referenced to a common average. Frontal and temporal channels were excluded due to poor signal quality.

C. *Static Classification*

Classification was performed using shrinkage LDA (sLDA) on sliding windows of low-frequency EEG features, employing the Ledoit-Wolf shrinkage for covariance regularization [20]. Binary labels for the continuous data were assigned following Crell et al. [21]. Windows of length w (from timepoint t_0 to t_0+w) were shifted in 0.0625 s steps ($1/f_s$). Using the motion capture data to extract the timepoint of movement onset t_{onset}, windows ending at $t_{onset}+d$ were labelled as *movement*, all others were labelled as *no movement*. The delay d incorporated post-onset information to reduce false positives (FPs). Hyperparameters ($w \in [0.5, 2.0]$ s; $d \in [0, w]$, step 0.1 s) were optimized per participant via 4-fold cross-validation on session 1 by maximizing the mean Matthews Correlation Coefficient (MCC). The final static model was retrained on session 1 with optimal parameters and applied to later sessions. The probability threshold p was determined on session 2 (0.1-0.9, step 0.1) to maximize MCC under the constraint of ≤ 1 false positive per minute (FP/min). Predictions within ±0.25 s of the true movement onset were counted as true positives (TP).

D. *Adaptive Classification*

a. *Adaptive Feature Normalization (FNorm)*

Poor generalization arises from EEG non-stationarities that shift feature distributions between training and test data [2]. A common strategy to address such covariate shifts is data normalization, which aligns these probability distributions [22]. We applied this using EMA filters to estimate the time-varying mean m_t and standard deviation s_t of the $(1\times n)$ feature vectors using exponentially decaying weights, following Hehenberger et al. [3], further referred to as *FNorm* strategy. At each time point t, the incoming feature vector x_t is used to update the estimates of m_t and s_t. Based on the estimates from the previous time step ($t-1$), the update rule for each component i is defined as follows:

$$m_t^{(i)} = (1-\eta)m_{t-1}^{(i)} + \eta x_t^{(i)} \tag{1}$$

$$s_t^{(i)} = \sqrt{(1-\eta){s_{t-1}^{(i)}}^2 + \eta\left(x_t^{(i)} - m_t^{(i)}\right)^2} \tag{2}$$

The smoothing parameter η weighs the contribution of the current feature vector on normalization. Initial estimates (m_0 and s_0) were taken from session 1. The smoothing parameter η was defined as

$$\eta = 1 - (1-p)^{\frac{1}{k}} \tag{3}$$

where k represents the number of observations whose cumulative weights account for a fraction p of the total EMA weights, i.e., the exponentially decaying coefficients that determine the contribution of past samples in the moving average. A participant-wise grid search on session 2 evaluated $p \in [10, 20]$ (step size 2) and $k \in [10, 70]$ (step size 5), selecting parameters that maximized MCC – λ·FP/min, with λ = 0.05.
The normalized feature vector was then calculated as:

$$\tilde{x}_t = (x_t - m_t)\Sigma_t^{-\frac{1}{2}} \tag{4}$$

with $$\Sigma_t^{-\frac{1}{2}} = \operatorname{diag}(s_t) = \begin{bmatrix} s_t^{(1)} & 0 & 0 \\ 0 & \ddots & 0 \\ 0 & 0 & s_t^{(n)} \end{bmatrix} \tag{5}$$

b. *Pooled Mean Adaptation (PMean)*

Another unsupervised adaptation strategy, following Vidaurre et al. [10,12], updates the classifier parameters directly. Test data from session 2 to 6 were normalized using session 1 statistics. We adapted the pooled class mean μ using EMA filters (see Eq. (1)). Updating μ continuously adjusts the classifier bias term b

$$\mu = (\mu_1 + \mu_2)/2 \tag{6}$$

$$b = w^T\mu \tag{7}$$

while keeping the weights w fixed. In this paper, this approach is abbreviated by *PMean*.

c. *Adaptive Pooled Mean and Sample Covariance (PMean+Cov)*

Extending pooled mean adaptation approach, which

10.3217/978-3-99161-093-9-031

adjusts only the bias term b while keeping the weights w fixed, we incorporated a covariance update mechanism to also adapt the weights w [10,12]. Every minute, buffered unlabelled samples were used to estimate second-order statistics and update the inverse covariance matrix Σ^{-1}_{t-1}, yielding an unsupervised adaptation scheme. Instead of estimating class-specific covariances, a global second-order moment $E[xx^T]$ was computed. The inverse covariance matrix was updated recursively using a Woodbury identity-based formulation, allowing efficient incorporation of the new batch statistics without explicit recomputation or inversion of the full covariance matrix. To ensure numerical stability, Tikhonov regularization via diagonal loading was applied by adding a small-scaled identity matrix to the covariance estimate (or its inverse during recursive updates). The weights w were then recomputed as:

$$w_t = \Sigma_t^{-1}(\mu_1 - \mu_2) \tag{8}$$

This allowed continuous adaptation of both the decision boundary and bias b while retaining the session 1 model as initialization. In contrast to Eq. (1), separate update coefficients η_μ and η_Σ were introduced for the pooled mean and covariance adaptation, respectively, and were determined via a grid search on session 2 with η_μ and η_Σ $\in [0, 0.25]$. We refer to this adaptation strategy as *PMean+Cov*.

d. *FP/min Control*

To minimize FP, a probability threshold p adaptation mechanism was applied. The threshold p was used to convert classifier output probabilities into binary decisions (prediction = 1 if $P(class=1) \geq p$, otherwise 0). Predictions were generated run by run, and FP/min were computed after each run. The probability threshold p was adjusted via a feedback rule based on the deviation from a predefined target (FP/min = 1): $p \leftarrow p + \alpha \cdot (\text{FP/min} - \text{target})$, where $\alpha = 0.01$. Updates were only applied when the deviation exceeded a tolerance margin and were constrained to a fixed range ($p \in [0.1, 0.9]$). The threshold was increased when FP/min exceeded the target and decreased otherwise. This threshold controller was applied across all adaptive methods as a shared control layer. However, it represents a supervised post-hoc mechanism and is not intended for real-time application. Nonetheless, it was included to demonstrate the ability of the adaptive methods to reduce FP under controlled evaluation conditions.

E. Statistical Analysis

Statistical comparisons between the static sLDA classifier and adaptive methods were performed using linear mixed-effects models (LMMs) to account for repeated measurements across participants and sessions. For each performance metric (MCC, TPR, FP/min), the metric value was modelled as a function of method and session, with participants included as a random effect. Session-wise performance slopes were derived using session number as a continuous predictor, representing average performance change per session and capturing temporal trends. Analyses were conducted separately for adaptive configurations with and without FP/min control. Within each session, pairwise contrasts between the static sLDA baseline and each adaptive method were computed from fixed effects. One-sided p-values were calculated in the expected direction of improvement (adaptive > static for MCC and TPR; adaptive < static for FP/min), reflecting the prior, hypothesis that adaptive updates improve performance under non-stationary conditions. Effect sizes were obtained from estimated contrasts normalized by the residual standard deviation of the model. P-values were corrected for multiple comparisons across sessions using the Benjamini-Hochberg procedure. To compare adaptive strategies, group-level analyses were conducted using analogous LMMs that included all strategies simultaneously. These models enabled direct statistical comparisons between adaptive methods, the static sLDA baseline, and their interaction with session, while accounting for multiple testing via false discovery rate.

RESULTS

The performance of the static sLDA and adaptive classification methods across sessions for the different metrics, with and without FP/min control, is shown in Fig. 1. Tables 1 and 2 summarize the averaged performance across sessions of the adaptive methods relative to the static sLDA baseline. Tab. 1 corresponds to Fig. 1A (without FP/min control), and Tab. 2 to Fig. 1B (with FP/min control). For FP/min, negative differences to the baseline are desirable. Tab. 3 reports the best-performing adaptive method per metric and control condition. Tab. 4 presents the session-wise slopes of the best adaptive methods compared to static sLDA baseline to evaluate stability across sessions.

10.3217/978-3-99161-093-9-031

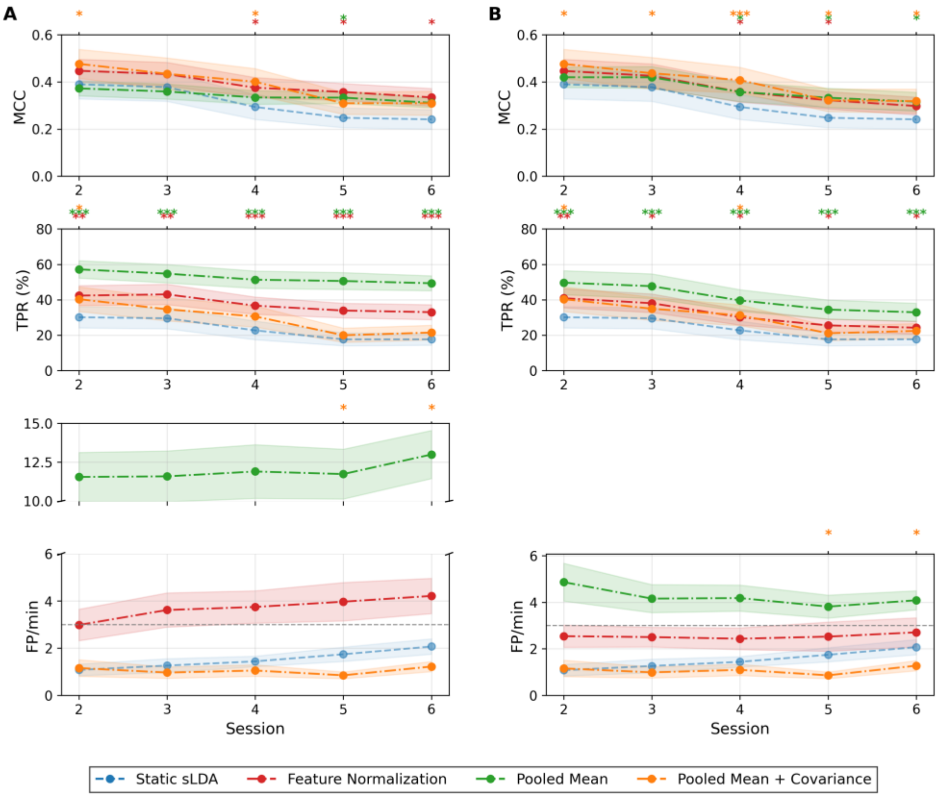

Figure 1: Performance metrics of the static sLDA classifier (blue) and the adaptive methods evaluated **A** without FP/min control and **B** with FP/min control. Color-coded asterisks denote statistically significant differences relative to the static baseline after Benjamini-Hochberg correction (* p<0.05, ** p<0.01, *** p<0.001).

Table 1: Performance metrics of each adaptive method without FP/min control. For both static and adaptive approaches, session-averaged values, minimum and maximum across sessions are reported along with the corresponding difference to the static baseline and the associated statistical significance corrected for multiple comparisons.

Metric	Method	Static			Adaptive			Delta			p-value
		Mean	Min	Max	Mean	Min	Max	Mean	Min	Max	
MCC	*FNorm*	0.31	0.24	0.39	0.39	0.33	0.45	0.08	0.06	0.11	< 0.001
	PMean				0.34	0.31	0.37	0.03	-0.02	0.09	< 0.05
	PMean +Cov				0.39	0.31	0.48	0.08	0.06	0.11	< 0.001
TPR	*FNorm*	23.5	17.6	30.09	37.77	32.97	43.02	14.27	12.25	16.29	< 0.001
	PMean				52.62	49.31	57.16	29.13	25.23	32.99	< 0.001
	PMean +Cov				29.37	19.94	40.33	5.87	2.34	10.24	< 0.05
FP/min	*FNorm*	1.52	1.08	2.07	3.71	2.98	4.21	2.19	1.91	2.36	> 0.05
	PMean				11.95	11.55	12.99	10.44	9.99	10.92	> 0.05
	PMean +Cov				1.05	0.85	1.22	-0.47	-0.89	0.08	> 0.05

Table 3: Best adaptive method compared to static sLDA classification for each metric either with or without FP/min control including statistical significance corrected for multiple comparisons.

Metric	FP/min Control	Best Method	p-value
MCC	False	*FNorm*	< 0.001
	True	*PMean+Cov*	< 0.001
TPR	False	*PMean*	< 0.001
	True	*PMean*	< 0.001
FP/min	False	*PMean+Cov*	> 0.05
	True	*PMean+Cov*	> 0.05

Table 4: Comparison of the best adaptive method and the static sLDA baseline in terms of robustness across sessions, evaluated with and without FP/min control. Session-wise performance slopes are reported.

Metric	FP/min Control	Best Method	Adaptive Slope	Static Slope
MCC	False	*PMean*	-0.015	-0.043
	True	*PMean*	-0.029	
TPR	False	*PMean*	-1.984	-3.684
	True	*FNorm*	-4.585	
FP/min	False	*PMean+Cov*	0.001	0.246
	True	*PMean*	-0.19	

10.3217/978-3-99161-093-9-031

Table 2: Performance metrics of each adaptive method with FP/min control. Session-averaged values (min-max), differences relative to the static baseline and associated statistical significance corrected for multiple comparisons.

Metric	Method	Static			Adaptive			Delta			p-value
		Mean	Min	Max	Mean	Min	Max	Mean	Min	Max	
MCC	*FNorm*	0.31	0.24	0.39	0.37	0.3	0.45	0.06	0.05	0.07	< 0.001
	PMean				0.37	0.32	0.42	0.06	0.03	0.09	< 0.001
	PMean +Cov				0.39	0.32	0.48	0.08	0.06	0.11	< 0.001
TPR	*FNorm*	23.5	17.6	30.09	31.74	24.19	40.85	8.24	6.56	10.76	< 0.001
	PMean				40.85	32.89	49.64	17.35	15.27	19.55	< 0.001
	PMean +Cov				29.98	21.04	40.33	6.48	3.44	10.24	< 0.001
FP/min	*FNorm*	1.52	1.08	2.07	2.54	2.43	2.71	1.02	0.64	1.46	> 0.05
	PMean				4.22	3.81	4.86	2.7	2.01	3.78	> 0.05
	PMean +Cov				1.07	0.86	1.27	-0.44	-0.88	0.08	> 0.05

DISCUSSION

Group-level LMMs revealed significant performance differences between adaptive strategies and the static sLDA baseline. Without FP/min control, the largest TPR increase was observed for *PMean* (+29.13%, $p \approx 10^{-53}$, see Tab. 1 and Fig. 1A), followed by *PMean* with FP control evaluated in the unconstrained setting (+17.35%, $p \approx 10^{-20}$, see Tab. 2 and Fig. 1B). All adaptive methods achieved positive MCC contrasts relative to static baseline. However, these improvements were accompanied by substantially elevated FPRs, particularly for *PMean* without FP/min control (+10.44 FP/min, $p > 0.05$, see Tab. 1 and Fig. 1A), reflecting a sensitivity-specificity trade-off. This may be partly explained by class imbalance, where no-movement samples dominate. *PMean* assumes balanced class contributions; under imbalance, the running mean can become biased toward the majority class, shifting the decision boundary and thereby increasing the FPR. Session-wise analyses indicated general performance declines over time across methods. Nevertheless, *PMean* showed less steep negative slopes for MCC and TPR compared to static decoding (see Tab. 4), suggesting improved robustness to temporal variability, although none of the methods achieved consistently stable performance across sessions.

With FP/min control, adaptive methods continued to outperform the static baseline in MCC. Notably, *PMean+Cov* achieved the largest MCC increase (+0.082, $p < 10^{-6}$), followed by *PMean* (+0.059, $p < 10^{-3}$), as shown in Tab. 2 and Fig. 1B. In contrast to the uncontrolled setting, FP/min control substantially constrained FPRs. *PMean+Cov* yielded the lowest FP/min and slightly fewer FPs than static decoding (-0.44 and -0.47 FP/min, see Fig. 1 and Tab. 2 and Tab. 1 respectively), although these reductions were not statistically significant after correction.

Together, these findings highlight a trade-off between TPR and FPR. Without FP/min control, *PMean* maximized TPR but at the cost of markedly increased FPs, limiting usability in real-time BCI applications. For example, in a speller operating at six characters per minute, FPRs above three per minute would result in roughly every second selection being incorrect, rendering the system impractical. Introducing FP/min control shifted adaptive methods toward a more practical operating point, preserving MCC gains while stabilizing FPRs. However, this controller relies on labelled feedback and is therefore not applicable in fully online scenarios.

Elevated FP/min in several adaptive strategies likely reflects increased sensitivity to non-stationary feature distributions. In addition, methods such as *PMean* may be sensitive to class imbalance, which is common in BCI settings, biasing the classifier toward more frequent classes. Among all methods, *PMean+Cov* achieved the best balance between sensitivity and specificity in both controlled and uncontrolled settings.

Overall, these findings demonstrate that simple adaptive extensions of linear models improve robustness to non-stationarity without requiring large datasets or computationally expensive deep learning architectures [6-9], making them suitable for low-trial EEG settings and real-time implantable BCIs.

CONCLUSION

This study investigated whether lightweight adaptation of sLDA improves decoding performance under non-stationary EEG conditions. The results support the hypothesis that adaptive extensions outperform static decoding. Among the evaluated strategies, pooled mean adaptation with covariance update (*PMean+Cov*) provided the best balance between sensitivity and FPRs and is therefore most suitable for real-time deployment.

As an alternative, feature normalization (*FNorm*) demonstrated stable performance across sessions in both TPR and FP/min. Although FP/min remained elevated compared to *PMean+Cov*, it was substantially lower than for *PMean* while maintaining consistent detection performance. *FNorm* may therefore be preferable when cross-session stability is the primary objective.

However, methods relying on global statistics, such as *PMean*, may be sensitive to class imbalance, inherent to BCI paradigms. Future work should therefore address

10.3217/978-3-99161-093-9-031

class imbalance during adaptation to improve robustness and reduce FPs.
Overall, these results indicate that simple adaptive extensions of linear models provide an effective, practical approach for improving robustness to non-stationarity in real-time BCI systems.

ACKNOWLEDGMENTS

This research was funded by the European Union's HORIZON-EIC-2021-PATHFINDER CHALLENGES program under grant agreement No 101070939 and by the Swiss State Secretariat for Education, Research and Innovation (SERI) under contract number 22.00198.

REFERENCES

[1] Birbaumer N, Ghanayim N, Hinterberger T, Iversen I, Kotchoubey B, Kübler A, et al. A spelling device for the paralysed. Nature. 1999 Mar;398(6725):297-8.

[2] Raza H, Rathee D, Zhou SM, Cecotti H, Prasad G. Covariate shift estimation based adaptive ensemble learning for handling non-stationarity in motor imagery related EEG-based brain-computer interface. Neurocomputing (Amst). 2019 May 28;343:154-66.

[3] Hehenberger L, Kobler RJ, Lopes-Dias C, Srisrisawang N, Tumfart P, Uroko JB, et al. Long-Term Mutual Training for the CYBATHLON BCI Race With a Tetraplegic Pilot: A Case Study on Inter-Session Transfer and Intra-Session Adaptation. Front Hum Neurosci. 2021 Feb 26;15:635777.

[4] Buttfield A, Ferrez PW, Millán J del R. Towards a robust BCI: error potentials and online learning. IEEE Trans Neural Syst Rehabil Eng. 2006 Jun;14(2):164–8.

[5] Vidaurre C, Schlögl A, Cabeza R, Scherer R, Pfurtscheller G. Adaptive on-line classification for EEG-based brain computer interfaces with AAR parameters and band power estimates. Biomed Tech (Berl). 2005 Nov;50(11):350–4.

[6] Wu D, Xu Y, Lu BL. Transfer learning for EEG-based brain–computer interfaces: A review of progress made since 2016. IEEE Trans Cogn Dev Syst. 2022 Mar;14(1):4–19.

[7] Wang X, Yang R, Huang M. An Unsupervised Deep-Transfer-Learning-Based Motor Imagery EEG Classification Scheme for Brain-Computer Interface. Sensors (Basel) [Internet]. 2022 Mar 14;22(6). Available from: http://dx.doi.org/10.3390/s22062241

[8] Liang S, Li L, Zu W, Feng W, Hang W. Adaptive deep feature representation learning for cross-subject EEG decoding. BMC Bioinformatics. 2024 Dec 31;25(1):393. Elsevier, Amsterdam, Netherlands (1999)

[9] Zhao H, Zheng Q, Ma K, Li H, Zheng Y. Deep Representation-Based Domain Adaptation for Nonstationary EEG Classification. IEEE Trans Neural Netw Learn Syst. 2021 Feb;32(2):535–45.

[10] Vidaurre C, Sannelli C, Müller KR, Blankertz B. Co-adaptive calibration to improve BCI efficiency. J Neural Eng. 2011 Apr;8(2):025009.

[11] Vidaurre C, Schlögl A, Cabeza R, Scherer R, Pfurtscheller G. Study of on-line adaptive discriminant analysis for EEG-based brain computer interfaces. IEEE Trans Biomed Eng. 2007 Mar;54(3):550–6.

[12] Vidaurre C, Kawanabe M, von Bünau P, Blankertz B, Müller KR. Toward unsupervised adaptation of LDA for brain-computer interfaces. IEEE Trans Biomed Eng. 2011 Mar;58(3):587–97.

[13] Wu S, Bhadra K, Giraud AL, Marchesotti S. Adaptive LDA Classifier Enhances Real-Time Control of an EEG Brain-Computer Interface for Decoding Imagined Syllables. Brain Sci [Internet]. 2024 Feb 21;14(3).

[14] Kapgate DD. Hybrid SSVEP + P300 brain-computer interface can deal with non-stationary cerebral responses with the use od adaptive classification. J Neurorestoratology. 2024 Jun;12(2):100109.

[15] Peck R, Van Ness J. The use of shrinkage estimators in linear discriminant analysis. IEEE Trans Pattern Anal Mach Intell. 1982 May;4(5):530–7.

[16] Sosulski J, Tangermann M. Introducing block-Toeplitz covariance matrices to remaster linear discriminant analysis for event-related potential brain-computer interfaces. J Neural Eng [Internet]. 2022 Nov 7;19(6). Available from: http://dx.doi.org/10.1088/1741-2552/ac9c98

[17] Egger J, Kostoglou K, Müller-Putz GR. Chrono-EEG dynamics influencing hand gesture decoding: a 10-hour study. Sci Rep. 2024 Aug 30;14(1):20247.

[18] Kobler, R. J., Sburlea, A. I., Lopes-Dias, C., Schwarz, A., Hirata, M., & Müller-Putz, G. R. (2020). Corneo-retinal-dipole and eyelid-related eye artifacts can be corrected offline and online in electroencephalographic and magnetoencephalographic signals. NeuroImage. 2020 Sep 1;218:117000.

[19] Perrin F, Pernier J, Bertrand O, Echallier JF. Spherical splines for scalp potential and current density mapping. Electroencephalogr Clin Neurophysiol. 1989 Feb;72(2):184–7.

[20] Ledoit, O., & Wolf, M. (2004). A well-conditioned estimator for large-dimensional covariance matrices. Journal of multivariate analysis, 88(2), 365-411.

[21] Crell MR, Kostoglou K, Suwandjieff P, Cruz JR da, Muller-Putz GR. A Non-Invasive, MRCP-Based BCI for Online Communication. IEEE Trans Neural Syst Rehabil Eng. 2026;34:1272–83.

[22] Apicella A, Isgrò F, Pollastro A, Prevete R. On the effects of data normalization for domain adaptation on EEG data. Eng Appl Artif Intell. 2023 Aug;123(106205):106205.